Timing-jitter reduction of passively mode-locked fiber laser with a carbon nanotube saturable absorber by optimization of cavity loss

Kan Wu,[1,*] Jia Haur Wong,[1] Ping Shum,[1] Desmond Rodney Chin Siong Lim,[1] Vincent Kwok Huei Wong,[1] Kenneth Eng Kian Lee,[1] Jianping Chen,[2] and E. D. Obraztsova[3]

[1]*School of Electrical & Electronic Engineering, Nanyang Technological University, Singapore 637553*
[2]*The State Key Laboratory on Advanced Optical Communication Systems and Networks, Shanghai Jiao Tong University, Shanghai, China 200051*
[3]*A. M. Prokhorov General Physics Institute, Russian Academy of Science, 39 Vavilov Street, Moscow, Russia, 119333*
**Corresponding author: wuka0002@ntu.edu.sg*

Received November 18, 2009; revised February 24, 2010; accepted February 25, 2010; posted March 3, 2010 (Doc. ID 120105); published March 31, 2010

We investigate the relationship between timing jitter and cavity loss of a passively mode-locked fiber ring laser with a carbon nanotube as a saturable absorber. It is the first time that we experimentally demonstrated the reduction of timing jitter by properly increasing laser cavity loss. The lowest timing jitter is achieved when the cavity loss is optimized. Theoretical analysis is in agreement with the experimental observations on the effect of cavity loss for the reduction of timing jitter. Moreover, it is experimentally shown that, at an optimal value of cavity loss, the timing jitter is reduced significantly by 24%, while the relative intensity noise increased by 4% only. © 2010 Optical Society of America

OCIS codes: 140.3510, 140.3538, 320.5550.

A mode-locked laser source with low timing jitter attracts intense attention because of its wide applications, e.g., high-resolution optical sampling [1], drift-free optical timing distribution [2], and frequency metrology [3]. von der Linde first evaluated the phase and intensity noise of a pulse train based on the rf spectrum [4]. Later, Haus and Meccozi investigated the quantum noise of mode-locked lasers [5]. Their theory was further developed by Namiki and Haus [6], Jiang *et al.* [7], and Paschotta [8]. Quantum-limited noise performance has been achieved in a stretched pulse-fiber laser by Namiki and Haus [6], semiconductor laser by Jiang *et al.* [7], and normal dispersive ytterbium fiber laser by Prochnow *et al.* [9], respectively. Meanwhile, various technologies have also been proposed to reduce the timing jitter. For example, Jiang *et al.* achieved 47 fs (10 Hz–10 MHz) jitter by inserting a 0.7 nm bandpass filter to limit Gordon–Haus jitter [7]. Chen *et al.* achieved 27 fs jitter (1 kHz–10 MHz) by adopting feedback control of the cavity length [10], and Gee *et al.* achieved subfemtosecond 0.66 fs jitter (0.9 Hz–1 MHz) by applying a slab-coupled optical waveguide amplifier and a phase-locked loop [11].

It is generally believed that a low cavity loss would result in low phase noise and timing jitters because of the reduction of spontaneous emission (SE). However, we first experimentally demonstrated that for passively mode-locked lasers with a carbon nanotube saturable absorber, the timing jitter can be minimized by properly increasing cavity loss. Theoretical analysis supports our experimental observations. Timing jitter coupled from the fluctuation of central wavelength of mode-locked state via dispersion can be suppressed by higher cavity loss (corresponding to higher cavity gain) through decreasing cavity relaxation time τ_p (defined below). The effect of cavity loss on the relative intensity noise (RIN) is also discussed.

A typical passively mode-locked fiber ring laser setup with a single-wall carbon nanotube (SWCNT) based saturable absorber is shown in Fig. 1. The SWCNT facilitates low self-starting pump power (18–28 mW) in this laser. The total cavity loss without additional attenuation is ~3.3 dB. The total cavity length is ~10.6 m, corresponding to a fundamental repetition rate of ~18.8 MHz. The length of a single-mode fiber is ~7 m with dispersion $-0.02\ \mathrm{ps}^2/\mathrm{m}$. The length of erbium-doped fiber is ~3.6 m with dispersion $0.01\ \mathrm{ps}^2/\mathrm{m}$. Thus the total dispersion is $\sim -0.1\mathrm{ps}^2$. An rf spectrum analyzer (Rohde & Schwarz FSUP26) is used to measure the phase-noise spectrum of the output pulse train from the passively mode-locked laser after a 2 GHz photodetector.

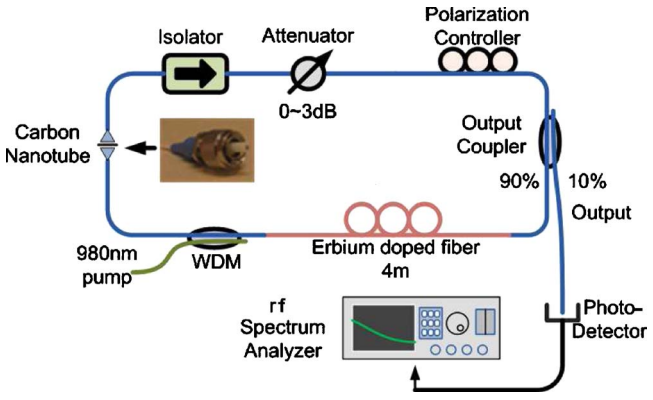

Fig. 1. (Color online) Experimental setup of a passively mode-locked fiber ring laser with a carbon nanotube as a saturable absorber.

 © 2010 Optical Society of America

We adopt von der Linde's method to measure the phase-noise spectrum [4]. For a noisy pulse train after the photodetector, the corresponding power spectrum density is derived as

$$P_V(f) = |\tilde{H}(f)|^2|\tilde{f}(f)|^2 \sum_{k=-\infty}^{+\infty} [\delta(f - kf_{rep}) + P_A(f - kf_{rep}) + 4\pi^2 k^2 P_J(f - kf_{rep})], \quad (1)$$

where $\tilde{H}(f)$ is the system response of detection equipment, $\tilde{f}(f)$ is the Fourier transform of a single pulse's intensity envelope, $\delta(f)$ is the delta function in frequency domain induced by periodic pulse train, f_{rep} is the fundamental repetition rate, k is the order of harmonics, and $P_A = |\tilde{A}(f)|^2$ and $P_J = |\tilde{J}(f)|^2$ are the power spectrum density of intensity noise $\tilde{A}(f)$ and timing noise $\tilde{J}(f)$, respectively. The displayed power value at frequency f_i in the rf spectrum analyzer is the integration of $P_V(f)$ within one resolution bandwidth. The phase-noise spectrum $L(f) \equiv 4\pi^2 P_J(f)$ can then be extracted by comparing fundamental component and high-order component (e.g., tenth harmonics).

Figure 2(a) shows the phase-noise spectra when different additional attenuation is added into the laser cavity with the polarization controller remaining unchanged. As shown, all four curves exhibit −20 dB/decade decrease at frequency $f > 8$ kHz, which is a typical characteristic of mode-locked lasers [9,12]. Compared with the original curve (black solid curve), the phase-noise spectrum (red dotted curve) decreases at low frequency and increases at high frequency when cavity loss is increased by 1 dB. When 2 dB attenuation is introduced, the phase-noise spectrum (gray solid curve) decreases further at low frequency and increases further at high frequency. However, the phase-noise spectrum (magenta dashed curve) displays dissimilar behavior when 3 dB attenuation is introduced; it increases at low frequency and remains nearly unchanged at high frequency compared with 2 dB case. This indicates that further increasing cavity loss will not improve the phase noise. Moreover, mode locking is unachievable if additional attenuation is greater than 3 dB. Figure 2(b) shows the timing jitters as calculated by $\Delta t = 1/(2\pi f_{rep})\sqrt{2\int_{f_{\min}}^{f_{\max}} L(f)df}$. The experimental error, with uncertainty of ~10%, arises from the fluctuation of measurements from the rf spectrum analyzer.

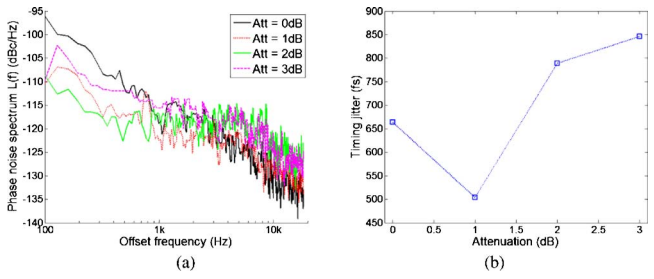

Fig. 2. (Color online) (a) Phase-noise spectrum with respect to different additional attenuation added into the cavity; (b) calculated timing jitters according to (a) with integration range of 100 Hz–20 kHz.

Owing to higher cavity loss, intracavity power is reduced, consequently weakening the nonlinear effects. This led to a change in phase delay that detunes the laser away from its most stable mode-locked state. By adjusting the cavity birefringence induced by the polarization controller, the change of phase delay can be compensated and a most stable state can be achieved. Figure 3(a) illustrates the optimal experimental results. Output powers are −6.6, −6.9, −8.0, and −7.9 dBm for 0–3 dB attenuation, respectively. The corresponding pump powers are 18, 23, 28, and 28 mW. As shown, the curves display nearly similar behaviors. The calculated timing jitters and corresponding optical spectra are shown in Fig. 3(b). The timing jitters at 2 and 3 dB attenuation have been improved. The minimum timing jitter is obtained at 1 dB attenuation, which is 24% smaller than the jitter at 0 dB attenuation. The spectral shifts are due to the combined effects of fiber birefringence and nonlinearity of the laser [13].

Haus and Mecozzi's model can be adopted to explain the experimental results [5] with some coefficients corrected by Paschotta [8]. The equation of quantum noise of mode-locked laser is given by

$$L(f) = (2\pi f_{rep})^2 \left[\frac{D^2 D_p}{T_R^2} \frac{1}{(2\pi f)^2((2\pi f)^2 + \tau_p^{-2})} + \frac{D_t}{(2\pi f)^2} \right], \quad (2)$$

where $D_p = 2/3 w_0 \tau^2 \theta 2g / T_R h\nu$ and $D_t = \pi^2\tau^2/6 w_0 \theta 2g / T_R h\nu$ are diffusion constants of quantum noise, representing the noise properties of offset frequency and timing, respectively; θ is the enhancement factor due to the incomplete inversion of the gain medium; $\tau_p = 3\pi^2 T_R \Delta f_g^2 \tau^2 / 2g$ is the relaxation time; D is the total group dispersion; T_R is the round-trip time; w_0 is the total energy in the cavity; g is the incremental gain per round trip; τ is the pulse duration; and Δf_g is the gain bandwidth. This equation indicates two mechanisms describing how SE causes timing jitter. The first term represents an indirect contribution to timing jitter coupled from the random shift of central frequency caused by SE via dispersion. The second term represents a direct contribution to timing jitter in time domain caused by SE.

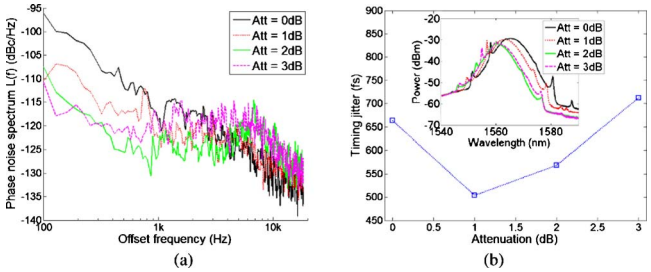

Fig. 3. (Color online) (a) Best results of a phase-noise spectrum with respect to different additional attenuation added into the cavity; (b) calculated timing jitter according to (a) with integration range of 100 Hz–20 kHz. Inset, corresponding optical spectra.

The second term dominates at high frequency, because the first term decreases by a factor of f^{-4}. Using parameter values described by our laser, the first term dominates at low frequency and is proportional to g^{-1}, while the second term is proportional to g. Therefore the phase-noise spectrum decreases when g increases. For a steady mode-locked laser, the gain compensates the cavity loss per round trip $e^{g}(1-\text{loss})=1$. Therefore increasing cavity loss is equivalent to increasing cavity gain. As g increases further, the difference between the first and second terms is reduced by a factor of g^2, with both terms finally becoming comparable in magnitude. Subsequently, the phase-noise spectrum will no longer decrease at low frequency with the increase of g.

The calculated timing jitters based on Haus and Meccozi's model are 6.40, 6.06, 6.55, and 6.75 fs with respect to 0 to 3 dB attenuation. It is clearly observed that a very similar behavior occurs. The discrepancy between experimental results and theoretical analysis is probably due to the coupling of intensity noise to timing noise. By comparing the value of relaxation peak in the phase noise spectrum in 2 dB curve in Fig. 3(a) and that in the RIN spectrum in 2 dB curve in Fig. 4(a) (discussed below), there exists an approximate −22 dB coupling ratio between them. The following timing jitter of 446, 102, 344, and 573 fs with respect to 0 to 3 dB attenuation are calculated by subtracting the coupling part. Additionally, the uncertainty in the exact excess noise factor and gain bandwidth of erbium-doped fiber under saturated conditions, may contribute an approximate factor of 10 [14]. Technical noise may also cause another factor of 3–5.

With $P_J(f)$ known, the RIN spectrum can be extracted from Eq. (1), as shown in Fig. 4(a). The RIN is shown in Fig. 4(b). It is observed that the RIN increases only 4% at 1 dB attenuation compared with 0 dB attenuation. We further verify our observations in a laser mode locked through nonlinear polarization rotation (NPR). As the NPR-based artificial saturable absorber exploits the fiber Kerr effect and is highly dependent on the pulse power, an increased cavity loss deters the laser from mode locking. Mode locking is unachievable using our 300 mW, 976 nm pump when an adaptor with typical 0.4 dB loss is inserted in the cavity. But we believe that our result is valid for those mode-locked lasers with similar material-based saturable absorbers, e.g. SESAMs [15] and Graphene [16].

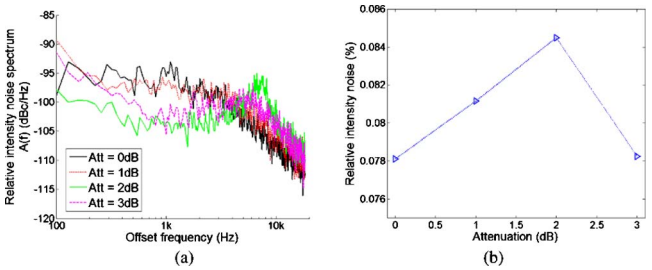

Fig. 4. (Color online) (a) Relative intensity noise spectrum with respect to different additional attenuation when best phase-noise performance is obtained in Fig. 3; (b) calculated RIN according to (a).

In conclusion, we experimentally demonstrated that the timing jitter of a passively mode-locked fiber ring laser with carbon nanotube saturable absorber can be improved by optimizing the cavity loss. A higher cavity loss assists in suppressing the coupling from a random shift of central frequency to the timing jitter. With proper increase in the cavity loss, the phase-noise spectrum decreases at low frequency and increases at high frequency, resulting in lower timing jitter. A further increase in cavity loss induces the phase-noise spectrum to increase at low frequency, causing timing jitter to increase as the direct effect of spontaneous emission on timing effect becomes dominant. We have demonstrated in our experiment that the timing jitter is reduced significantly by 24%, while relative intensity noise increased by only 4%.

The authors thank Mr. E. J. R. Kelleher of the Imperial College, London, UK for the discussion on the single-wall carbon nanotube samples and Dr. Paschotta of RP Photonics Consulting GmbH for useful suggestions.

References

1. G. C. Valley, Opt. Express **15**, 1955 (2007).
2. J. Kim, J. A. Cox, J. Chen, and F. X. Kartner, Nat. Photonics **2**, 733 (2008).
3. J. J. McFerran, W. C. Swann, B. R. Washburn, and N. R. Newbury, Opt. Lett. **31**, 1997 (2006).
4. D. von der Linde, Appl. Phys. Lett. **39**, 201 (1986).
5. H. A. Haus and A. Mecozzi, IEEE J. Quantum Electron. **29**, 983 (1993).
6. S. Namiki and H. A. Haus, IEEE J. Quantum Electron. **33**, 649 (1997).
7. L. A. Jiang, M. E. Grein, E. P. Ippen, C. McNeilage, J. Searls, and H. Yokoyama, Opt. Lett. **27**, 49 (2002).
8. R. Paschotta, Appl. Phys. B **79**, 153 (2004).
9. O. Prochnow, R. Paschotta, E. Benkler, U. Morgner, J. Neumann, D. Wandt, and D. Kracht, Opt. Express **17**, 15525 (2009).
10. J. Chen, J. W. Sickler, P. Fendel, E. P. Ippen, F. X. Kärtner, T. Wilken, R. Holzwarth, and T. W. Hänsch, Opt. Lett. **33**, 959 (2008).
11. S. Gee, S. Ozharar, F. Quinlan, J. J. Plant, P. W. Juodawlkis, and P. J. Delfyett, IEEE Photonics Technol. Lett. **19**, 498 (2007).
12. J. Kim, J. Chen, J. Cox, and F. X. Kärtner, Opt. Lett. **32**, 3519 (2007).
13. H. Xu, D. Lei, S. Wen, X. Fu, J. Zhang, Y. Shao, L. Zhang, H. Zhang, and D. Fan, Opt. Express **16**, 7169 (2008).
14. H. Byun, D. Pudo, J. Chen, E. P. Ippen, and F. X. Kärtner, Opt. Lett. **33**, 2221 (2008).
15. U. Keller, K. J. Weingarten, F. X. Kartner, D. Kopf, B. Braun, I. D. Jung, R. Fluck, C. Honninger, N. Matuschek, and J. A. derAu, IEEE J. Quantum Electron. **2**, 435 (1996).
16. H. Zhang, Q. Bao, D. Tang, L. Zhao, and K. Loh, Appl. Phys. Lett. **95**, 141103 (2009).